

## Ternary Inclusion Complexes of $\gamma$ -Cyclodextrin with Resorufin and Organic Cations in Aqueous Solution

Sanyo Hamai

Department of Chemistry, Faculty of Education and Human Studies, Akita University,  
1-1 Tegata Gakuen-machi, Akita 010-8502

Received January 5, 2007; E-mail: hamai@ipc.akita-u.ac.jp

Molecular interactions of an organic anion, resorufin (Res), with  $\gamma$ -cyclodextrin ( $\gamma$ -CD) and several organic cations were investigated by means of absorption and fluorescence spectroscopy. A 1:1 inclusion complex is formed between  $\gamma$ -CD and Res. In addition, Res forms a 1:1 organic cation–organic anion complex with 1,1'-diheptyl-4,4'-bipyridyl dibromide (DHB) and 1,1'-dimethyl-4,4'-bipyridyl dibromide (DMB), although Res does not form an organic cation–organic anion complex with trimethyloctylammonium bromide (TMOA). The  $\gamma$ -CD–Res inclusion complex forms a ternary inclusion complex with TMOA, DHB, and DMB. The equilibrium constant for the formation of the 1:1:1  $\gamma$ -CD–Res–TMOA inclusion complex is nearly the same as that of the 1:1:1  $\gamma$ -CD–Res–DHB inclusion complex. On the other hand, the equilibrium constant for the formation of the 1:1:1  $\gamma$ -CD–Res–DMB inclusion complex is significantly less than that of 1:1:1  $\gamma$ -CD–Res–DHB inclusion complex. These findings suggest that the long alkyl-chain in the organic cations examined promotes the formation of a ternary inclusion complex of Res.

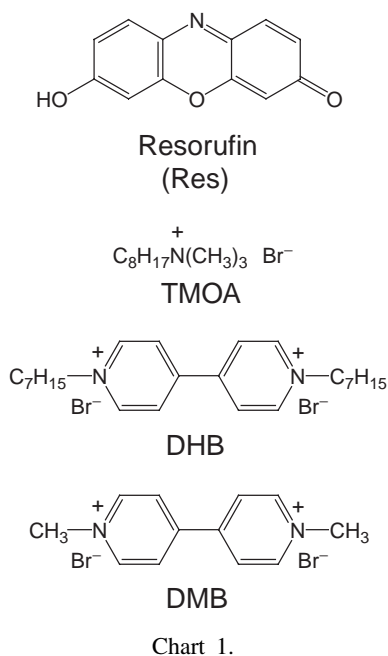
Cyclodextrins (CDs) are cyclic oligosaccharides, which are composed of more than five D-glucopyranose residues.<sup>1</sup> Commercially available  $\alpha$ -,  $\beta$ -, and  $\gamma$ -CDs have six, seven, and eight D-glucopyranose residues, respectively. Because CDs have a relatively hydrophobic cavity, an organic molecule of appropriate dimensions can be incorporated into the CD cavity to form a 1:1 inclusion complex.<sup>2</sup> In several cases, two CD molecules accommodate a single guest molecule to form a 2:1 CD–guest inclusion complex.<sup>3–6</sup> It is known that two guest molecules of the same or different kinds are bound to the CD cavity to form a 1:2 CD–guest inclusion complex or a 1:1:1 CD–guest 1–guest 2 inclusion complex.<sup>7–17</sup> At high concentrations, organic dyes, such as Methyl Orange and Methylene Blue, readily dimerize in aqueous solution.<sup>10,11,18–20</sup> The dimer of these dyes does not dissociate to the monomers, and the dimer is bound to the  $\gamma$ -CD cavity to form a 1:2 CD–dye inclusion complex. In some cases, organic dyes dimerize to a greater extent within the  $\gamma$ -CD cavity rather than in aqueous solution.

When two guest molecules are located together within the CD cavity, they are expected to more or less interact with each other; in the case that the two guests are an electron donor and an electron acceptor, charge-transfer interactions may occur between the two guests. Within the  $\gamma$ -CD cavity, sodium 1-naphthylacetate forms an electron donor–electron acceptor (EDA) complex with picric acid, although the EDA complex is not formed in bulk water.<sup>21,22</sup> A ternary inclusion complex is formed among  $\beta$ -CD, 1-pyrenesulfonate (or pyrene), and aniline; the two different guest molecules produce an EDA complex within the  $\beta$ -CD cavities.<sup>23</sup> It is thought that hydrophobic interactions take place between CD and a guest molecule possessing a hydrophobic group, such as an alkyl chain. Electrostatic interactions have been suggested between a 2,6-bis(1-pyridiniummethyl)naphthalene cation and naphthalenedicarboxylates located within the  $\gamma$ -CD cavity.<sup>9</sup> For ion-association

reactions of organic cations with organic anions, Takayanagi et al. have shown that there are many types of interactions: electrostatic interaction, hydrophobic interaction, stacking of aromatic moieties, and so on.<sup>24–26</sup>

It has been reported that thionine forms an organic cation–organic anion complex with 2-naphthalenesulfonate in aqueous solution.<sup>10</sup> In addition, the thionine–2-naphthalenesulfonate complex is incorporated into the  $\gamma$ -CD cavity to form a 1:1:1  $\gamma$ -CD–thionine–2-naphthalenesulfonate inclusion complex.<sup>10</sup> An organic cation–organic anion complex is formed between tetrakis(4-sulfonatophenyl)porphyrin (TSPP) and trimethyloctylammonium bromide (TMOA).<sup>17</sup> Tetrakis(4-carboxyphenyl)porphyrin (TCPP) and hematoporphyrin also form an organic cation–organic anion complex with 1,1'-diheptyl-4,4'-bipyridyl dibromide (DHB).<sup>14,17</sup> The TSPP–TMOA and TCPP–DHB complexes are bound to the  $\gamma$ -CD cavity to form ternary inclusion complexes. For hematoporphyrin, a similar ternary inclusion complex with  $\beta$ -CD has been suggested. An octyl group in TMOA and a heptyl group in DHB seem to play an important role in the formation of the  $\gamma$ -CD–TSPP–TMOA and  $\gamma$ -CD–TCPP–DHB inclusion complexes, respectively.

In the inclusion complexes of porphyrin derivatives, such as TSPP and TCPP, the CD cavity accommodates only a part of a large porphyrin molecule. Consequently, most of the porphyrin molecule resides outside the CD cavity. Taking into account the above structural features of the porphyrin derivatives, the molecular interactions, which contribute to the formation of the ternary inclusion complex, may operate outside as well as inside the CD cavity. In the ternary inclusion complex of  $\gamma$ -CD with tetrakis(4-N-methylpyridyl)porphyrin (TMPyP) and disodium phthalate (DSP), a DSP molecule, which is located outside the  $\gamma$ -CD cavity, associates with a TMPyP molecule bound to the  $\gamma$ -CD cavity.<sup>27</sup> In the case of the ternary inclusion



complexes including a porphyrin derivative, therefore, the analyses for the origin of the molecular interactions may be complicated.

For ternary inclusion complexes including an organic cation–organic anion complex, few studies have been made on the interactions in the formation of the ternary inclusion complex as well as the interactions between an organic cation and an organic anion in aqueous solution. To clarify the molecular interactions regarding the formation of the ternary inclusion complexes, we selected resorufin (Res) as a relatively small, simple organic anion, which is expected to be almost thoroughly buried within the CD cavity. As organic cations, TMOA, DHB, and 1,1'-dimethyl-4,4'-bipyridyl dibromide (DMB), which have an alkyl group, were selected. Thus, using electronic absorption and fluorescence spectroscopy, we have examined whether or not the ternary inclusion complexes are formed among  $\gamma$ -CD, Res, and the organic cations (TMOA, DHB, and DMB) as well as whether or not the organic cation–organic anion complexes are formed between Res and these organic cations.

### Experimental

Resorufin (Res), trimethyloctylammonium bromide (TMOA), 1,1'-diheptyl-4,4'-bipyridyl dibromide (DHB), and 1,1'-dimethyl-4,4'-bipyridyl dibromide (DMB) were obtained from Tokyo Chemical Industry Co., Ltd. and used as received (Chart 1).  $\gamma$ -Cyclodextrin ( $\gamma$ -CD) purchased from Wako Pure Chemical Industries, Ltd. was used without further purification.

Buffers ( $2.5 \times 10^{-3}$  mol dm $^{-3}$  of NaHCO $_3$  and  $1.4 \times 10^{-3}$  mol dm $^{-3}$  of NaOH) of pH 10.2 were used throughout this work, except for the titration experiments. Aqueous solution of Res, which was used for the preparation of sample solutions, was prepared by submerging Res crystals in water for a few days.

Absorption spectra were recorded on a Shimadzu UV-2450 UV–vis spectrophotometer. Fluorescence spectra were taken with a Shimadzu RF-501 spectrofluorometer equipped with a cooled Hamamatsu R-943 photomultiplier. The fluorescence spectra were

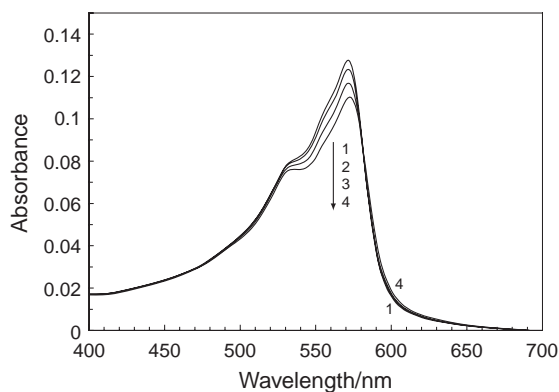


Fig. 1. Absorption spectra of Res ( $2.5 \times 10^{-6}$  mol dm $^{-3}$ ) in pH 10.2 buffers containing various concentrations of  $\gamma$ -CD. Concentration of  $\gamma$ -CD: (1) 0, (2)  $1.0 \times 10^{-3}$ , (3)  $3.0 \times 10^{-3}$ , and (4)  $1.0 \times 10^{-2}$  mol dm $^{-3}$ .

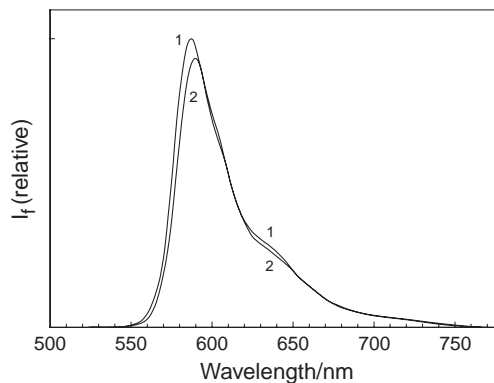


Fig. 2. Fluorescence spectra of Res ( $1.0 \times 10^{-6}$  mol dm $^{-3}$ ) in pH 10.2 buffers in the absence and presence of  $\gamma$ -CD ( $1.0 \times 10^{-2}$  mol dm $^{-3}$ ).  $\lambda_{\text{ex}} = 500$  nm.

corrected for the spectral response of the fluorometer. Spectroscopic measurements were made at  $25 \pm 0.1$  °C.

### Results and Discussion

**Inclusion Complexation of  $\gamma$ -CD with Res in Aqueous Solution.** The absorption maximum of Res in acidic solution was located at about 470 nm, whereas the absorption maximum in alkaline solution was at about 570 nm. In alkaline solution, Res is in an anionic form, because a hydroxy group of Res is deprotonated. From titration experiments using the absorbance at 571 nm and the fluorescence intensity at 585 nm,  $pK_a$  and apparent  $pK_a^*$  values were estimated to be 6.11 and 6.80, respectively. At around pH 10, therefore, Res in the ground and excited states exists as an anion. Thus, the spectroscopic measurements throughout this work were made at pH 10.2, where Res is in an anionic form.

Figure 1 shows absorption spectra of Res in pH 10.2 buffers containing various concentrations of  $\gamma$ -CD. As  $\gamma$ -CD is added to the Res solution, the absorption maximum of Res is reduced in intensity. This finding indicates the formation of an inclusion complex of  $\gamma$ -CD with Res. Figure 2 exhibits fluorescence spectra of Res in pH 10.2 buffers in the absence and presence of  $\gamma$ -CD ( $1.0 \times 10^{-2}$  mol dm $^{-3}$ ). Upon the addition

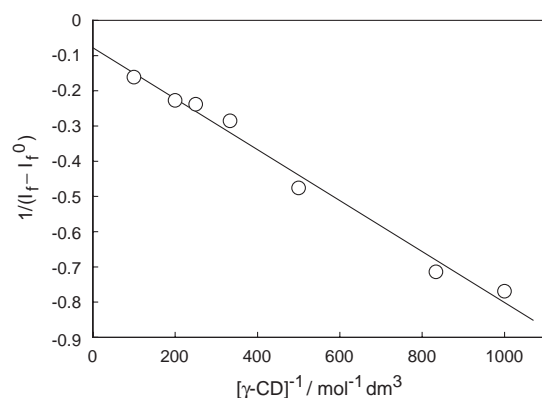
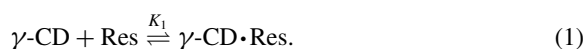


Fig. 3. Double-reciprocal plot for Res ( $1.0 \times 10^{-6}$  mol dm $^{-3}$ ) in pH 10.2 buffers containing  $\gamma$ -CD.  $\lambda_{\text{ex}} = 540$  nm.  $\lambda_{\text{obs}} = 585$  nm.

of  $\gamma$ -CD, the fluorescence maximum is decreased in intensity accompanied by a slight shift to longer wavelengths, indicating the formation of the  $\gamma$ -CD–Res inclusion complex.



Here,  $K_1$  is the equilibrium constant for the formation of the 1:1  $\gamma$ -CD–Res inclusion complex ( $\gamma\text{-CD}\cdot\text{Res}$ ). When the  $\gamma$ -CD–Res inclusion complex has a 1:1 stoichiometry, a double-reciprocal plot holds for the fluorescence intensity and the  $\gamma$ -CD concentration:

$$1/(I_f - I_f^0) = 1/a + 1/(aK_1[\gamma\text{-CD}]), \quad (2)$$

where  $I_f$ ,  $I_f^0$ , and  $a$  are the fluorescence intensity in the presence of  $\gamma$ -CD, the fluorescence intensity in the absence of  $\gamma$ -CD, and an experimental constant, respectively. From the plot based on Eq. 2, a  $K_1$  value of  $110 \pm 20$  mol $^{-1}$  dm $^3$  is evaluated (Fig. 3). The good linearity ( $R = 0.9929$ ) of the observed fluorescence data confirms the 1:1 stoichiometry of the  $\gamma$ -CD–Res inclusion complex. From the absorbance data in Fig. 1, the  $K_1$  value has been estimated to be  $170 \pm 30$  mol $^{-1}$  dm $^3$ , which is comparable to the  $K_1$  value evaluated from the fluorescence intensity change.

For Res in  $\gamma$ -CD solution, the fluorescence intensity is represented by the sum of the fluorescence intensities of free Res and the  $\gamma$ -CD–Res inclusion complex.

$$\begin{aligned} I_f &= b[\text{Res}] + c[\gamma\text{-CD}\cdot\text{Res}] \\ &= (b + cK_1[\gamma\text{-CD}])([\text{Res}]_0 / (1 + K_1[\gamma\text{-CD}])), \end{aligned} \quad (3)$$

where  $b$  and  $c$  are experimental constants that include the fluorescence quantum yields of free Res and the  $\gamma$ -CD–Res inclusion complex, respectively, and  $[\text{Res}]_0$  is the initial concentration of Res. The  $K_1$  value has already been determined from the double-reciprocal plot. From a simulation (Fig. S1) employing Eq. 3, the ratio ( $c/b$ ) of the experimental constant for the  $\gamma$ -CD–Res inclusion complex to that for free Res has been estimated to be 0.765 at an excitation wavelength of 460 nm.

**Interactions of  $\gamma$ -CD with Res in Solution Containing TMOA.** The absorption spectrum of Res in the presence of TMOA ( $1.0 \times 10^{-2}$  mol dm $^{-3}$ ) was almost the same as that in the absence of TMOA. In addition, the  $\text{p}K_a$  value of Res in the presence of TMOA ( $1.0 \times 10^{-2}$  mol dm $^{-3}$ ) was estimat-

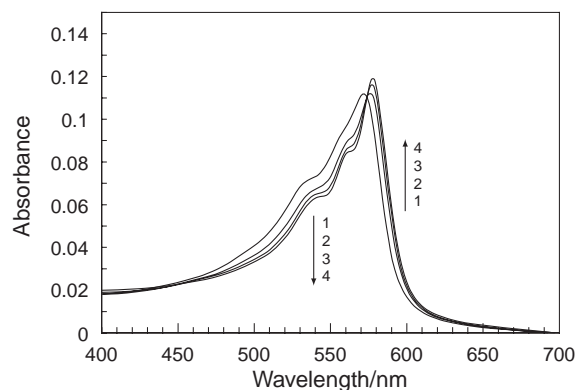
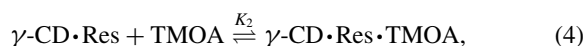


Fig. 4. Absorption spectra of Res ( $2.3 \times 10^{-6}$  mol dm $^{-3}$ ) in pH 10.2 buffers containing TMOA ( $1.0 \times 10^{-2}$  mol dm $^{-3}$ ) and various concentrations of  $\gamma$ -CD. Concentration of  $\gamma$ -CD: (1) 0, (2)  $1.0 \times 10^{-3}$ , (3)  $3.0 \times 10^{-3}$ , and (4)  $1.0 \times 10^{-2}$  mol dm $^{-3}$ .

ed to be 6.76, which is identical to the  $\text{p}K_a$  value (6.80) obtained from the titration in the absence of TMOA within experimental error. Consequently, there are little or no interactions between Res and TMOA, that is, an organic cation–organic anion complex is not formed between Res and TMOA. Figure 4 illustrates absorption spectra of Res in pH 10.2 buffers containing a fixed concentration ( $1.0 \times 10^{-2}$  mol dm $^{-3}$ ) of TMOA and various concentrations of  $\gamma$ -CD. When the  $\gamma$ -CD concentration is increased, the absorption maximum of Res shifts to longer wavelengths, accompanied by an enhancement of the absorbance at the maximum. The absorption spectral change in the presence of TMOA is different from that in the absence of TMOA (Fig. 1), suggesting the formation of a ternary inclusion complex among  $\gamma$ -CD, Res, and TMOA.

Harada et al. have reported that inclusion complexes are formed between poly(ethylene glycol) and not  $\beta$ -CD but  $\alpha$ -CD.<sup>28</sup> Poly(propylene glycol), which has methyl side-chains, forms inclusion complexes with  $\beta$ -CD and  $\gamma$ -CD, although  $\alpha$ -CD does not form inclusion complexes with poly(propylene glycol) of any molecular weight. It is most likely that an inclusion complex between  $\gamma$ -CD and TMOA scarcely forms, because the alkyl chain of TMOA does not fit into the  $\gamma$ -CD cavity.

Figure 5 shows fluorescence spectra of Res in pH 10.2 buffers containing a fixed concentration ( $1.0 \times 10^{-2}$  mol dm $^{-3}$ ) of TMOA and various concentrations of  $\gamma$ -CD. The Res fluorescence is quenched by the addition of  $\gamma$ -CD, indicating the formation of a ternary inclusion complex of  $\gamma$ -CD, Res, and TMOA. Taking into account the cavity size of  $\gamma$ -CD, the ternary  $\gamma$ -CD–Res–TMOA inclusion complex most likely has a 1:1:1 stoichiometry:



where  $K_2$  is the equilibrium constant for the formation of the 1:1:1  $\gamma$ -CD–Res–TMOA inclusion complex ( $\gamma\text{-CD}\cdot\text{Res}\cdot\text{TMOA}$ ).

The fluorescence intensity of the Res solution containing  $\gamma$ -CD and TMOA is represented by the sum of the fluorescence intensities of free Res, the  $\gamma$ -CD–Res inclusion complex, and the 1:1:1  $\gamma$ -CD–Res–TMOA inclusion complex:

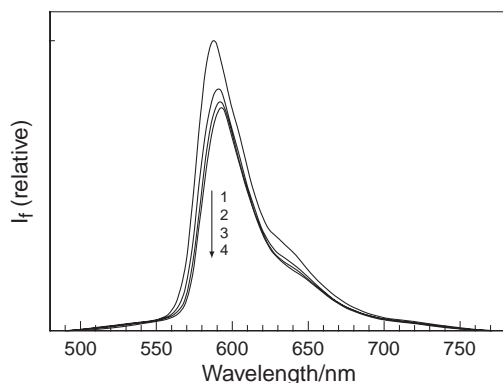
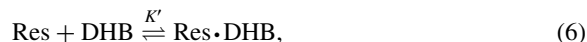


Fig. 5. Fluorescence spectra of Res ( $1.0 \times 10^{-6} \text{ mol dm}^{-3}$ ) in pH 10.2 buffers containing TMOA ( $1.0 \times 10^{-2} \text{ mol dm}^{-3}$ ) and various concentrations of  $\gamma$ -CD. Concentration of  $\gamma$ -CD: (1) 0, (2)  $1.0 \times 10^{-3}$ , (3)  $3.0 \times 10^{-3}$ , and (4)  $1.0 \times 10^{-2} \text{ mol dm}^{-3}$ .  $\lambda_{\text{ex}} = 460 \text{ nm}$ .

$$I_f = d[\text{Res}] + e[\gamma\text{-CD}\cdot\text{Res}] + f[\gamma\text{-CD}\cdot\text{Res}\cdot\text{TMOA}] \\ = (d + eK_1[\gamma\text{-CD}] + fK_1K_2[\gamma\text{-CD}][\text{TMOA}])[\text{Res}]_0 \\ / (1 + K_1[\gamma\text{-CD}] + K_1K_2[\gamma\text{-CD}][\text{TMOA}]), \quad (5)$$

where  $d$ ,  $e$ , and  $f$  are experimental constants that include the fluorescence quantum yields of free Res, the 1:1  $\gamma$ -CD-Res inclusion complex, and the 1:1:1  $\gamma$ -CD-Res-TMOA inclusion complex, respectively. The  $K_1$  value and the coefficient ratio ( $e/d = c/b$ ) have previously been evaluated. Using these evaluated values, the fluorescence intensity of Res in solution containing a fixed concentration ( $1.0 \times 10^{-2} \text{ mol dm}^{-3}$ ) of TMOA has been simulated as a function of the  $\gamma$ -CD concentration. Figure 6 exhibits the best fit simulation curve (solid curve), for which the  $K_2$  value is presumed to be  $1560 \text{ mol}^{-1} \text{ dm}^3$  (Table 1). The simulation curve fits the observed fluorescence intensities, confirming the existence of the 1:1:1  $\gamma$ -CD-Res-TMOA inclusion complex. If the  $\gamma$ -CD-Res-TMOA inclusion complex is not formed (only the  $\gamma$ -CD-Res inclusion complex is formed), the fluorescence intensity of Res is expressed by Eq. 3. In this case, the simulation curve (dotted curve), which is also shown in Fig. 6, does not reproduce the observed fluorescence data, supporting the formation of the 1:1:1  $\gamma$ -CD-Res-TMOA inclusion complex.

**Interactions of  $\gamma$ -CD with Res in Solution Containing DHB.** Figure 7 illustrates absorption spectra of Res in pH 10.2 buffers in the absence (spectrum 1) and presence (spectrum 2) of DHB. In the presence of DHB, the absorption-band intensity of Res is reduced with a slight band shift to longer wavelengths. This is due to the formation of an organic cation-organic anion complex between Res and DHB.



where  $K'$  is the equilibrium constant for the formation of the 1:1 Res-DHB complex (Res·DHB).

When DHB was added, the Res fluorescence was strongly quenched, indicating the formation of the Res-DHB complex. From a double-reciprocal plot concerning the fluorescence intensity and the DHB concentration, the  $K'$  value was evaluated to be  $117 \pm 3 \text{ mol}^{-1} \text{ dm}^3$  (Table 1 and Fig. S2). The excellent linearity ( $R = 1.000$ ) of the observed fluorescence data con-

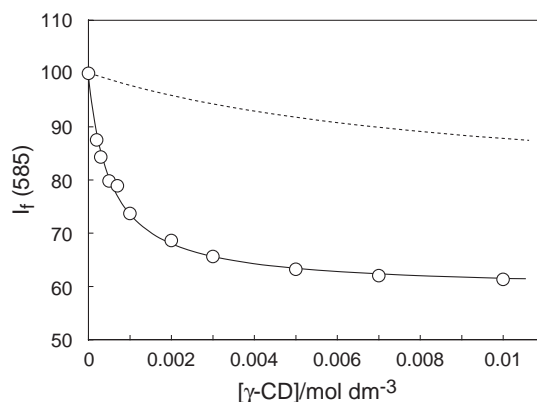


Fig. 6. Simulation for the observed fluorescence intensities of Res ( $1.0 \times 10^{-6} \text{ mol dm}^{-3}$ ) in pH 10.2 buffers containing TMOA ( $1.0 \times 10^{-2} \text{ mol dm}^{-3}$ ) and various concentrations of  $\gamma$ -CD. The best fit simulation curve (solid curve) for the formation of the 1:1:1  $\gamma$ -CD-Res-TMOA inclusion complex was calculated with the evaluated  $K_1$  value of  $110 \text{ mol}^{-1} \text{ dm}^3$  and the  $e/d$  value of 0.765, under the assumptions of  $d = 9.93 \times 10^7$ ,  $f = 5.84 \times 10^7$ , and  $K_2 = 1560 \text{ mol}^{-1} \text{ dm}^3$ . The best fit simulation curve (dotted curve) based on the scheme not involving the formation of the 1:1:1  $\gamma$ -CD-Res-TMOA inclusion complex was calculated with the evaluated  $K_1$  value of  $110 \text{ mol}^{-1} \text{ dm}^3$  and the  $e/d$  value of 0.765.  $\lambda_{\text{ex}} = 460 \text{ nm}$ .  $\lambda_{\text{obs}} = 585 \text{ nm}$ .

Table 1. Values of  $K_2$ ,  $K_3$ , and  $K'$  for TMOA, DHB, and DMB

	$K_2/\text{mol}^{-1} \text{ dm}^3$	$K_3/\text{mol}^{-1} \text{ dm}^3$	$K'/\text{mol}^{-1} \text{ dm}^3$
TMOA	1560	—	—
DHB	1430	1340	$117 \pm 3$
DMB	44.6	40.9	$120 \pm 20$

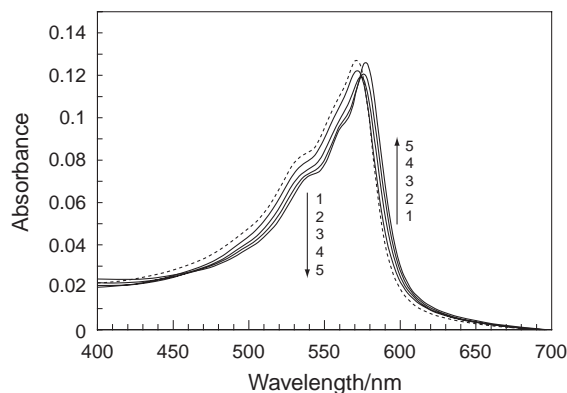


Fig. 7. Absorption spectra of Res ( $2.5 \times 10^{-6} \text{ mol dm}^{-3}$ ) in pH 10.2 buffers containing DHB ( $3.0 \times 10^{-3} \text{ mol dm}^{-3}$ ) except for spectrum 1) and various concentrations of  $\gamma$ -CD. For spectrum 1, the DHB concentration is zero. Concentration of  $\gamma$ -CD: (1) 0, (2) 0, (3)  $1.0 \times 10^{-3}$ , (4)  $3.0 \times 10^{-3}$ , and (5)  $1.0 \times 10^{-2} \text{ mol dm}^{-3}$ .

firmed the 1:1 stoichiometry for the Res-DHB complex. There is a static quenching of the Res fluorescence by DHB, because the Res-DHB complex is formed in the ground state of Res. If

dynamic quenching contributes to the fluorescence quenching, a Stern–Volmer plot for the Res solution containing DHB should be curved. However, the Stern–Volmer plot (Fig. S3) has exhibited an excellent linearity ( $R = 1.000$ ), suggesting that dynamic quenching of the Res fluorescence by DHB is negligible. As in the case of the  $\gamma$ -CD–Res system, the simulation for the observed fluorescence intensity afforded the coefficient ratio of the fluorescence intensity of the Res–DHB complex to that of free Res; the coefficient ratio thus estimated was zero, implying the complete quenching of the Res fluorescence by the formation of the Res–DHB complex.

It has been reported that DHB scarcely forms an inclusion complex with  $\gamma$ -CD, due to the  $\gamma$ -CD cavity being too large to closely include a hydrophobic heptyl-chain of DHB.<sup>29</sup> In the presence of DHB ( $3.0 \times 10^{-2} \text{ mol dm}^{-3}$ ), the addition of  $\gamma$ -CD results in a red-shift of the absorption maximum and its intensity enhancement (Fig. 7). This absorption spectral change upon the addition of  $\gamma$ -CD to the Res solution containing DHB is similar to that containing TMOA. Consequently, it is most likely that the 1:1:1  $\gamma$ -CD–Res–DHB inclusion complex is formed. The fluorescence intensity of Res in solution containing  $\gamma$ -CD and DHB is expressed as the sum of the fluorescence intensities of free Res, the 1:1 Res–DHB complex, the 1:1  $\gamma$ -CD–Res inclusion complex, and the 1:1:1  $\gamma$ -CD–Res–DHB inclusion complex ( $\gamma$ -CD•Res•DHB):

$$\begin{aligned} I_f &= g[\text{Res}] + h[\text{Res} \cdot \text{DHB}] + i[\gamma\text{-CD} \cdot \text{Res}] \\ &\quad + j[\gamma\text{-CD} \cdot \text{Res} \cdot \text{DHB}] \\ &= (g + hK'[\text{DHB}] + iK_1[\gamma\text{-CD}] \\ &\quad + jK_1K_2[\gamma\text{-CD}][\text{DHB}])([\text{Res}]_0 \\ &\quad / (1 + K'[\text{DHB}] + K_1[\gamma\text{-CD}] + K_1K_2[\gamma\text{-CD}][\text{DHB}])). \quad (7) \end{aligned}$$

Here,  $g$ ,  $h$ ,  $i$ , and  $j$  are experimental constants that include the fluorescence quantum yields of free Res, the 1:1 Res–DHB complex, the 1:1  $\gamma$ -CD–Res inclusion complex, and the 1:1:1  $\gamma$ -CD–Res–DHB inclusion complex, respectively. The values of  $K'$ ,  $K_1$ ,  $h/g$  ( $=0$ ), and  $i/g$  ( $=0.756$ ) have previously been estimated. Using these values, the simulation has been performed as a function of the  $\gamma$ -CD concentration. Figure 8 depicts the best fit simulation curve (solid curve) calculated using a  $K_2$  value of  $1430 \text{ mol}^{-1} \text{ dm}^3$  (Table 1). The simulation curve reproduces the observed intensity data, confirming the existence of the 1:1:1  $\gamma$ -CD–Res–DHB inclusion complex. Although DHB forms the organic cation–organic anion complex with Res, the  $K_2$  value ( $1430 \text{ mol}^{-1} \text{ dm}^3$ ) for DHB is very close to the  $K_2$  value for TMOA ( $1560 \text{ mol}^{-1} \text{ dm}^3$ ), which does not form an organic cation–organic anion complex with Res. This finding suggests that a relatively long alkyl chain plays a critical role in the formation of the ternary inclusion complex, and that, in the ground state of the  $\gamma$ -CD–Res–DHB inclusion complex, there are little or no interactions between the aromatic rings of Res and DHB. The invasion of the hydrophobic heptyl-group of DHB into the  $\gamma$ -CD cavity may sterically prohibit the approach of the aromatic moiety of Res to the pyridine ring(s) of DHB. This is supported by the similarity in the absorption spectral changes of Res in  $\gamma$ -CD solutions containing TMOA and DHB; the sharpening and enhancement of the absorption band shown in Fig. 7 provide evidence for little or no interactions between the aromatic rings of Res in the

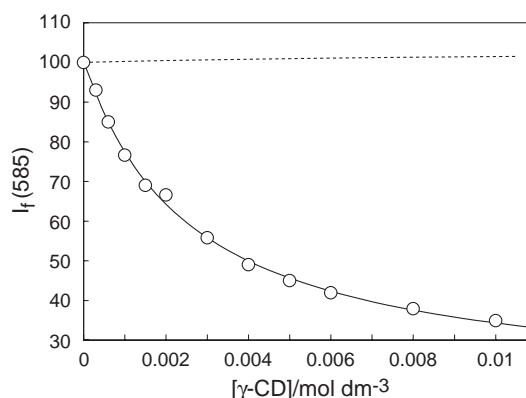


Fig. 8. Simulation for the observed fluorescence intensities of Res ( $1.0 \times 10^{-6} \text{ mol dm}^{-3}$ ) in pH 10.2 buffers containing DHB ( $3.0 \times 10^{-3} \text{ mol dm}^{-3}$ ) and various concentrations of  $\gamma$ -CD. The best fit simulation curve (solid curve) for the formation of the  $\gamma$ -CD–Res–DHB inclusion complex was calculated using the evaluated  $K_1$ ,  $K'$ ,  $h/g$ , and  $i/g$  values of  $110 \text{ mol}^{-1} \text{ dm}^3$ ,  $117 \text{ mol}^{-1} \text{ dm}^3$ , 0, and 0.756, respectively, and an assumed  $K_2$  value of  $1430 \text{ mol}^{-1} \text{ dm}^3$ . The best fit simulation curve (dotted curve) based on the scheme not involving the formation of the 1:1:1  $\gamma$ -CD–Res–DHB inclusion complex was calculated with the evaluated  $K_1$ ,  $K'$ ,  $h/g$ , and  $i/g$  values of  $110 \text{ mol}^{-1} \text{ dm}^3$ ,  $117 \text{ mol}^{-1} \text{ dm}^3$ , 0, and 0.756, respectively.  $\lambda_{\text{ex}} = 460 \text{ nm}$ .  $\lambda_{\text{obs}} = 585 \text{ nm}$ .

ground state and DHB within the  $\gamma$ -CD cavity. From the simulation shown in Fig. 8, the  $j$  value is estimated to be  $9.88 \times 10^{-9} \text{ mol}^{-1} \text{ dm}^3$ , which is very close to zero. Consequently, the fluorescence quenching of Res occurs in the  $\gamma$ -CD–Res–DHB inclusion complex, suggesting that the excited state of Res is dynamically quenched by a DHB molecule bound to the  $\gamma$ -CD cavity.

Under the assumption that the  $\gamma$ -CD–Res–DHB inclusion complex has not been formed (the  $\gamma$ -CD–Res inclusion complex and the Res–DHB complex alone have been produced), a simulation has been performed, using the estimated values of  $K'$ ,  $K_1$ ,  $h/g$ , and  $i/g$ . The simulation curve (dotted curve) thus obtained is also shown in Fig. 8. For this reaction scheme, the simulation curve does not fit the observed fluorescence intensity data. Consequently, this result supports the existence of the 1:1:1  $\gamma$ -CD–Res–DHB inclusion complex.

The equilibrium for the formation of the 1:1:1  $\gamma$ -CD–Res–DHB inclusion complex from  $\gamma$ -CD and the Res–DHB complex is represented by



where  $K_3$  is the equilibrium constant for the formation of the 1:1:1  $\gamma$ -CD–Res–DHB inclusion complex from  $\gamma$ -CD and the Res–DHB complex. The relationship among the equilibrium constants is given by

$$K_3 = K_1K_2/K'. \quad (9)$$

From Eq. 9, the  $K_3$  value for DHB is calculated to be  $1340 \text{ mol}^{-1} \text{ dm}^3$ , which is ten-times greater than the  $K_1$  value. This means that the  $\gamma$ -CD cavity encapsulates a Res molecule complexed with a DHB molecule more than a free Res molecule.

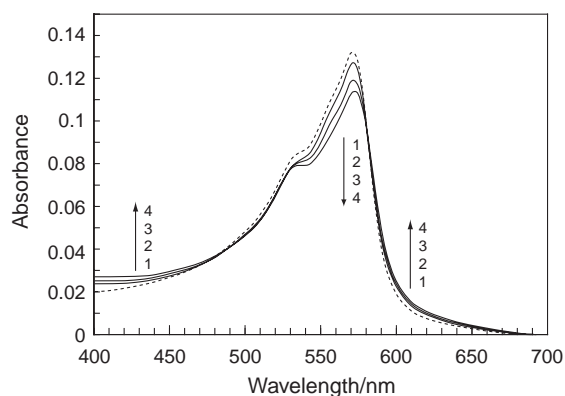


Fig. 9. Absorption spectra of Res ( $2.5 \times 10^{-6} \text{ mol dm}^{-3}$ ) in pH 10.2 buffers containing DMB ( $3.0 \times 10^{-3} \text{ mol dm}^{-3}$ ) except for spectrum 1) and various concentrations of  $\gamma$ -CD. For spectrum 1, the DMB concentration is zero. Concentration of  $\gamma$ -CD: (1) 0, (2) 0, (3)  $3.0 \times 10^{-3}$ , and (5)  $1.0 \times 10^{-2} \text{ mol dm}^{-3}$ .

Consequently, the heptyl chain of DHB is most likely embedded in the void space inside the  $\gamma$ -CD cavity accommodating a Res molecule. The space-regulating effects of the hydrophobic heptyl-chain may accelerate the formation of the ternary inclusion complex of Res. In DHB, two ends of a bipyridyl moiety are connected with a heptyl chain. Consequently, two heptyl chains of DHB do not seem to be simultaneously included into the  $\gamma$ -CD cavity accommodating a Res molecule due to steric hindrance.

**Interactions of  $\gamma$ -CD with Res in Solution Containing DMB.** When DMB is added to a Res solution, an absorption spectral change similar to that for the Res–DHB system is observed (Fig. 9), suggesting that an organic cation–organic anion complex is formed between Res and DMB. In the presence of DMB, the Res fluorescence was considerably quenched, indicating the formation of the Res–DMB complex. From the double-reciprocal plot involving the fluorescence intensity and the DMB concentration, the  $K'$  value for the formation of the 1:1 Res–DMB complex was estimated to be  $120 \pm 20 \text{ mol}^{-1} \text{ dm}^3$ , which is nearly the same as the  $K'$  value for DHB (Table 1). This finding suggests that the alkyl chain of DMB (DHB) exerts no effects on the formation of the Res–DMB (DHB) complex. As in the case of DHB (Fig. 7), the absorbance at the absorption maximum decreases upon the addition of DMB to the Res solution without  $\gamma$ -CD, accompanied by a slight shift of the absorption band to longer wavelengths (Fig. 9).

It is most likely that there are little or no interactions between  $\gamma$ -CD and DMB, because DMB, which has methyl chains, is more hydrophilic than DHB, which has heptyl chains. When  $\gamma$ -CD is added to a Res solution containing DMB ( $3.0 \times 10^{-2} \text{ mol dm}^{-3}$ ), the absorbance at the absorption maximum further decreases, accompanied by a slight red-shift of the absorption band (Fig. 9). The absorption spectral change is most likely due to the formation of the  $\gamma$ -CD–Res–DMB inclusion complex, although the absorption spectral change for DMB is different from that for DHB. The difference in the absorption spectral change between the  $\gamma$ -CD–Res–DMB and  $\gamma$ -CD–Res–DHB systems seems to arise from the different envi-

ronment around a Res molecule located within the  $\gamma$ -CD cavity; in the  $\gamma$ -CD–Res–DMB inclusion complex, the aromatic moiety of Res interacts with the pyridine ring(s) of DMB, whereas, in the  $\gamma$ -CD–Res–DHB inclusion complex, a Res molecule interacts with a hydrophobic heptyl-chain of DHB within the  $\gamma$ -CD cavity. The decrease in the absorbance at the absorption maximum by the addition of  $\gamma$ -CD to the Res solution containing DMB may suggest that charge-transfer interactions between Res and DMB to some extent contribute to the formation of the  $\gamma$ -CD–Res–DMB inclusion complex. A short methyl group in DMB cannot stabilize the ternary inclusion complex through the hydrophobic interactions of the methyl group with  $\gamma$ -CD.

Upon the addition of  $\gamma$ -CD to a Res solution containing DMB, the Res fluorescence was quenched, indicating the formation of the  $\gamma$ -CD–Res–DMB inclusion complex. The  $K_2$  value for DMB was evaluated to be  $44.6 \text{ mol}^{-1} \text{ dm}^3$  from a simulation similar to that for DHB. This  $K_2$  value for DMB is only about 3% of the  $K_2$  value for DHB, suggesting that the alkyl chain in the organic cations plays a critical role in the stability of the ternary inclusion complexes of Res. From Eq. 9, the  $K_3$  value for DMB is estimated to be  $40.9 \text{ mol}^{-1} \text{ dm}^3$ , which is less than 40% of the  $K_1$  value. In contrast to the Res–DHB complex, the Res–DMB complex is incorporated to a lesser extent into the  $\gamma$ -CD cavity than a free Res molecule. The difference in the inclusion behavior between the Res–DHB and Res–DMB complexes is due to the difference in the length of the alkyl chain between DHB and DMB.

## Conclusion

In pH 10.2 buffer, the organic anion Res does not form an organic cation–organic anion complex with TMOA, whereas Res forms organic cation–organic anion complexes with DHB and DMB. The Res fluorescence has completely been quenched by the formation of the organic cation–organic anion complexes with DHB and DMB. In bulk water, electrostatic interactions most likely promote the formation of the organic cation–organic anion complex between Res and DHB (or DMB). A 1:1 inclusion complex is formed between  $\gamma$ -CD and Res. The value of  $K_2$  for the formation of the ternary inclusion complex of  $\gamma$ -CD with Res and TMOA is nearly the same as that of  $\gamma$ -CD with Res and DHB. This suggests that, in the ternary inclusion complexes of TMOA and DHB, an alkyl chain of TMOA (DHB) is bound to the  $\gamma$ -CD cavity accommodating a Res molecule. On the other hand, the  $K_2$  value for DMB is significantly less than that for DHB, suggesting that the long alkyl chain in the bipyridyl cations plays a critical role in the stabilization of the ternary inclusion complex of Res.

## Supporting Information

Simulation for the evaluation of a  $c/b$  value (Fig. S1); double-reciprocal plot for the evaluation of a  $K'$  value of DHB (Fig. S2); Stern–Volmer plot of the Res fluorescence quenched by DHB (Fig. S3). These materials are available free of charge on the Web at: <http://www.csj.jp/journals/bcsj/>.

## References

- 1 W. Saenger, *Angew. Chem., Int. Ed. Engl.* **1980**, *19*, 344.
- 2 M. L. Bender, M. Komiyama, *Cyclodextrin Chemistry*,

Springer-Verlag, New York, **1978**.

- 3 H.-R. Park, B. Mayer, P. Wolschann, G. Kohler, *J. Phys. Chem.* **1994**, 98, 6158.
- 4 E. K. Fraiji, Jr., T. R. Cregan, T. C. Werner, *Appl. Spectrosc.* **1994**, 48, 79.
- 5 J. M. Ribó, J.-A. Farrera, M. L. Valero, A. Virgili, *Tetrahedron* **1995**, 51, 3705.
- 6 G. M. Escandar, *Analyst* **1999**, 124, 587.
- 7 R. L. Schiller, J. H. Coates, S. F. Lincoln, *J. Chem. Soc., Faraday Trans. 1* **1984**, 80, 1257.
- 8 C. Retna Raj, R. Ramaraj, *J. Photochem. Photobiol., A* **1999**, 122, 39.
- 9 W. H. Tan, T. Ishikura, A. Maruta, T. Yamamoto, Y. Matsui, *Bull. Chem. Soc. Jpn.* **1998**, 71, 2323.
- 10 S. Hamai, *Bull. Chem. Soc. Jpn.* **2000**, 73, 861.
- 11 S. Hamai, H. Satou, *Bull. Chem. Soc. Jpn.* **2000**, 73, 2207.
- 12 J. M. Shuette, T. T. Ndou, A. M. de la Pena, S. Mukundou, Jr., I. M. Warner, *J. Am. Chem. Soc.* **1993**, 115, 292.
- 13 X. Shen, M. Belletête, G. Durocher, *Langmuir* **1997**, 13, 5830.
- 14 S. Hamai, *Bull. Chem. Soc. Jpn.* **2002**, 75, 2371.
- 15 S. Hamai, *Supramol. Chem.* **2004**, 16, 113.
- 16 K. Kano, I. Takenoshita, T. Ogawa, *J. Phys. Chem.* **1982**, 86, 1833.
- 17 S. Hamai, Y. Sasaki, T. Hori, A. Takahashi, *J. Inclusion Phenom. Macrocyclic Chem.* **2006**, 54, 67.
- 18 R. J. Clarke, J. H. Coates, S. F. Lincoln, *Carbohydr. Res.* **1984**, 127, 181.
- 19 H. Hirai, N. Toshima, S. Uenoyama, *Bull. Chem. Soc. Jpn.* **1985**, 58, 1156.
- 20 C. Lee, Y. W. Sung, J. W. Park, *J. Phys. Chem. B* **1999**, 103, 893.
- 21 N. Kobayashi, A. Ueno, T. Osa, *J. Chem. Soc., Chem. Commun.* **1981**, 340.
- 22 N. Kobayashi, R. Saito, A. Ueno, T. Osa, *Makromol. Chem.* **1983**, 184, 837.
- 23 S. Hamai, *J. Phys. Chem.* **1988**, 92, 6140.
- 24 T. Takayanagi, E. Wada, S. Motomizu, *Analyst* **1997**, 122, 57.
- 25 T. Takayanagi, E. Wada, M. Oshima, S. Motomizu, *Bull. Chem. Soc. Jpn.* **1999**, 72, 1785.
- 26 T. Takayanagi, N. Ban, E. Wada, M. Oshima, S. Motomizu, *Bull. Chem. Soc. Jpn.* **2000**, 73, 669.
- 27 S. Hamai, *J. Inclusion Phenom. Macrocyclic Chem.*, in press.
- 28 A. Harada, M. Okada, J. Li, M. Kamachi, *Macromolecules* **1995**, 28, 8406.
- 29 M. Kodaka, *J. Am. Chem. Soc.* **1993**, 115, 3702.